Cation Modulation of Bicelle Size and Magnetic Alignment as Revealed by Solid-State NMR and Electron Microscopy

Alexandre Arnold, Thomas Labrot, Reiko Oda, and Erick J. Dufourc
Institut Européen de Chimie et Biologie, Ecole Polytechnique, Bordeaux-Pessac 33607, France

ABSTRACT The influence of salts (KCl, NaCl, $CaCl_2$, and $MgCl_2$) on bicelles (bilayered micelles) made of dimyristoylphosphatidylcholine (DMPC, molar fraction X = 78%) and dicaproylphosphatidylcholine (DCPC) was investigated by solid-state ^{31}P- and ^{2}H NMR as well as by freeze-fracture electron microscopy. Sizes were determined from ^{2}H- and ^{31}P NMR on the basis of a model that incorporated a planar bilayer and a (half-torus) curved rim representing the DMPC and DCPC regions of the bicelle, respectively. Good agreement was shown with sizes determined independently from freeze-fracture electron microscopy images. In the presence of K^+ and Na^+, bicelles have diameters of ~300 Å while in the presence of Ca^{2+} and Mg^{2+}; their diameter increases to ~500 Å. Bicelle magnetic alignment is considerably improved by the presence of salts. The optimum salt concentration for such an effect ranges from 50 to 200 mM. Bicelles are magnetically aligned for temperatures roughly ranging from 30°C to 40°C with monovalent cations; this range is slightly extended in the presence of divalent salts. In this temperature range, the dynamics of the long-chain hydrocarbon region of the bicelle (leading to a bicelle thickness of 38 Å) and of water is about the same independently of cation nature and concentration. However, at higher temperatures, considerable differences in water dynamics are observed between systems with monovalent and divalent cations. In these conditions, the system consists of a mixture of micelles and extended bilayers, which show residual macroscopic alignment in the magnetic field.

INTRODUCTION

Probing the structure and dynamics of peptides or proteins embedded in membranes is greatly improved when the orientation of the lipid matrix can be controlled. For instance, model membranes can be sandwiched between microscope glass plates. Interaction with the surface is such that the bilayer plane becomes parallel to the plate surface. However, the poor hydration control in these samples renders this model inadequate to study protein-lipid interactions in natural systems. In contrast, monolayer studies (Langmuir films) provide good hydration conditions, but their conclusions are bound to air-water interface systems. Among the many membrane systems that can be macroscopically aligned, one specific type of magnetically alignable model membrane known as bicelles (bilayer micelle) has drawn particular interest in recent years (Gabriel and Roberts, 1984, 1986; Sanders and Prestegard, 1990). Bicelle systems are composed of a binary mixture of long-chain (C14-C18) and short-chain (C6-C8) phospholipids or bile salt analogs. For lipid molar fractions (long/short) between 0.5 and 0.9, the water mixture of these two lipids is supposed to form disk-like aggregates that align with their bilayer normal perpendicular to the magnetic fields (Katsaras et al., 1997; Prosser et al., 1996). The disk model is, however, subject to controversy. Nieh and coworkers (Nieh et al., 2001) propose that the disk model can account only for the small angle neutron scattering (SANS) data at 25°C and that a perforated lamellar phase would be present at 45°C. Other groups favor the disk model in the temperature range 30–40°C where magnetic alignment has occurred (Raffard et al., 2000; Sternin et al., 2001). However, to our knowledge and for molar ratios of the two lipids ranging from 60% to 90%, there is no direct evidence for such disk-like particles. One must nonetheless mention electron microscopy images for bicelle systems with lipid ratios lower than 50% and where disks of 21-nm diameter are seen (Glover et al., 2001). The domain where C14-C6 phospholipid systems align as a function of hydration, ratio of two lipids, temperature, and presence or absence of K^+ has been determined by Raffard et al. (2000). Interestingly, alignment with magnetic field was improved by addition of small amounts of KCl to the solution. On the other hand, trivalent lanthanide ions such as Yb^{3+}, Tm^{3+}, and Eu^{3+} were reported to promote a change in disk orientation by 90° with respect to the magnetic field (Prosser et al., 1996, 1998). However, the influence of monovalent and divalent cations of biological relevance such as Na^+, Ca^{2+}, and Mg^{2+} has not been reported.

Bicellar particle size is thought to range from 10 to 100 nm and depends on the experimental molar ratio of the two lipids, $r_{long/short}$ = [long-chain lipid]/[short-chain lipid]. A model to calculate the bicelle size has been proposed (Picard et al., 1999; Sanders and Schwonek, 1992; Vold and Prosser, 1996). It is based upon the interfacial curvature of assemblies of long- and short-chain lipids. When dispersed in water independently, short-chain (C_N, with $N \leq 10$) lipids tend to form aggregates with high curvature such as micelles whereas long-chain (C_N, with $N \geq 12$) lipids self-assemble to form systems with a curvature close to zero such as in extended bilayers. To form disk-like structures

Submitted March 21, 2002, and accepted for publication June 20, 2002.

Address reprint requests to Dr. Erick J. Dufourc, IECB-Polytechnique, 16 Avenue Pey Berland, 33607 Pessac cedex, France. Tel.: +33-5-57962218; Fax: +33-5-57962218; E-mail: erick.dufourc@iecb-polytechnique.u-bordeaux.fr.

© 2002 by the Biophysical Society

0006-3495/02/11/2667/14 $2.00

with mixtures of the two above lipids, it was supposed that the long-chain lipids form the discoidal part of the bicelle and the short-chain lipids are located at the disc edge of a half-torus geometry. In this way they are preventing the long hydrophobic alkyl chains from contact with water.

The aim of this work is three-fold: 1) to visualize bicelles with electron microscopy using the freeze-fracture technique, 2) to assess the disk model for bicelles by solid-state NMR (the sizes as obtained from the microscopy images will be compared with those obtained from NMR), and 3) to determine the influence of the nature, charge, and concentration of biologically relevant monovalent and divalent cations such as K^+, Na^+, Ca^{2+}, and Mg^{2+} on bicelle thickness, size, and macroscopic alignment in a magnetic field.

Theoretical background

Geometrical considerations for the calculation of bicelle NMR spectra have been presented elsewhere (Picard et al., 1999; Vold and Prosser, 1996). Bicelle ^{31}P NMR spectra of dimyristoylphosphatidylcholine (DMPC)/dicaproylphosphatidylcholine (DCPC) mixtures are always composed of two lines that have been assigned to the disc and half-torus lipids, respectively. We will outline just what is needed for the present work. Time-dependent (FID) ^{31}P NMR signals can be written as:

$$g(t) = e^{i\omega t}e^{-t/T_2}, \tag{1}$$

where

$$\omega = \omega_{iso} - \frac{2\Delta\sigma}{3}\frac{(3\cos^2\beta - 1)}{2}S. \tag{2}$$

In Eq. 1, T_2 stands for the spin-spin relaxation time (homogeneous broadening). In Eq. 2, $\Delta\sigma$ represents the chemical shift anisotropy, and S is a general order parameter that can be expanded according to Douliez et al. (1995) and contains all time-dependent angular averages. β gives the orientation of the principal axis of motion, n, with respect to the magnetic field z-direction, B_0. The NMR frequencies given by Eq. 2 are weighted according to a static angular distribution function, $p(\beta)$, describing the probability of finding normal orientation at an angle β with respect to B_0. $p(\beta) = \sin\beta$ for randomly oriented samples (large vesicles) and may be more complex for cylindrical distributions or when vesicle deformation is taken into account (Pott et al., 1995). In the case of bicelles that orient with the disc plane parallel to the magnetic field, $\beta = 90°$. $p(\beta) = 1$ for a perfectly aligned bicelles sample. In the case of bicelles that may be misaligned with respect to the magnetic field, $p(\beta)$ can be simply modeled by a Gaussian function defined as:

$$p(\beta) = \frac{1}{\eta\sqrt{2\pi}}e^{-(\beta-\beta_0)^2/2\eta^2}, \tag{3}$$

where η represents the Gaussian width, also called mosaicity (mosaic spread) and $\beta_0 = 90°$. In other words, the means

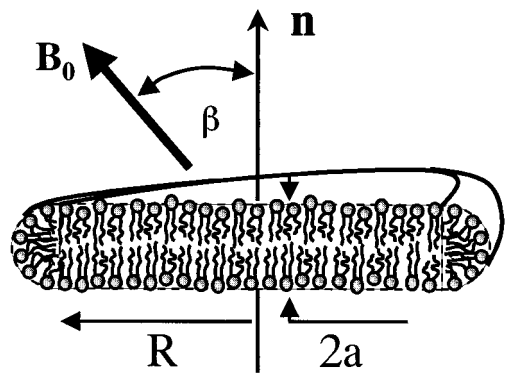

FIGURE 1 Schematic representation of a bicelle of diameter $2(R + a)$ and thickness $2a$. β is the angle between the normal to the bicelle plane and the magnetic field direction.

of the distribution is such that the normal to the bicelles plane is perpendicular to the magnetic field. It is important here to emphasize that our model is very crude and that application of the Gaussian distribution is valid only in the limit of fast exchange. That is, for a perfectly aligned sample, the diffusion of molecules in the disk and in the half-torus are fast enough to yield only a single, sharp, symmetric, Lorentzian line for each of the environments (the disk and the torus). So the bicelles spectrum is composed of two symmetrical sharp lines, which are experimentally observed with almost perfectly aligned samples. Also, such diffusion processes must be very fast, typically in the nanosecond to microsecond time scale. There are certainly limitations to this modeling, particularly a time-dependant Gaussian distribution could have been used. However, we wanted the simplest analysis that, although crude, correctly accounts for experimental spectra (vide infra). The FID is calculated by considering that the bicelle can be modeled (Fig. 1) as a disk of bilayer thickness $2a$ and of radius R, on one part, and by half a torus covering the disk rim and defined by the section diameter $2a$ and the radius R, on the other part. The FIDs for the torus and the disk contributions, $g_T(t)$ and $g_D(t)$, are calculated according to Eq. 2, where ω_{iso} is assigned to the isotropic chemical shift relative to 85% H_3PO_4 and $\Delta\sigma$ to the chemical shift anisotropy of fluid-phase phosphatidylcholines obtained from lipid dispersions (~45 ppm). The general order parameter, $0 \le S \le 1$, is adjusted to match the experimental frequencies, found for the disc and the half-torus resonance. The total FID is obtained by adding the weighted individual contributions, $a_T g_T(t) + a_D g_D(t)$, where a_T is the external area of the half-torus and a_D that of the upper plus lower disks:

$$a_T = 2\pi a(\pi R + 2a); \quad a_D = 2\pi R^2 \tag{4}$$

By introducing $q = a_D/a_T$ the bicelle diameter can be expressed as:

$$\Phi = aq[\pi + (\pi^2 + 8/q)^{1/2}] + 2a \tag{5}$$

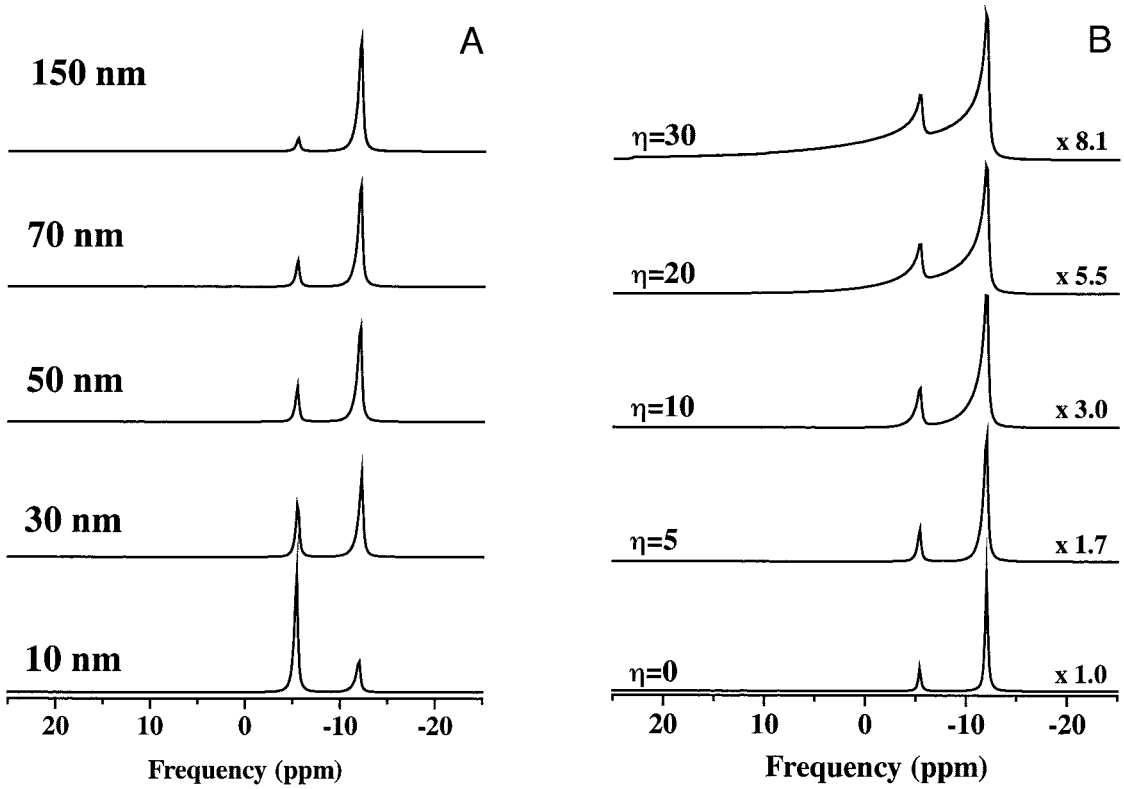

FIGURE 2 (*A*) Calculated ^{31}P NMR bicelle spectra for various bicelle diameters. Input parameters are: $\Delta\sigma = -7.3$ kHz (-45 ppm), isotropic chemical shift $= -0.5$ ppm, Lorentzian (homogeneous) linewidth $= 50$ Hz, Gaussian mosaicity $= 5°$, $S_{DMPC} = 0.836$, $S_{DCPC} = 0.393$, and bilayer thickness $= 40$ Å. Bicelle diameter is indicated on spectra. Spectra are normalized to the same spectral area. (*B*) Calculated ^{31}P NMR bicelle spectra for various mosaicities. Input parameters are as in *a* except bicelle diameter $= 700$ Å. Gaussian mosaicity is indicated on the left. Because spectral area is constant, the vertical scale was multiplied (numbers on right) to show spectral details.

Fourier transformation of FIDs leads to ^{31}P NMR spectra. Fig. 2 *a* shows calculated bicelles spectra as a function of bicelles diameter. It can be seen that NMR can be very sensitive, provided the above hypotheses are fulfilled, to probe bicelle sizes. The Fig. 2 *b* shows spectral simulations for various Gaussian widths. The increase of η results in a characteristic nonsymmetrical line shape toward high chemical shifts values.

MATERIALS AND METHODS

Chemicals

Synthetic DMPC, DCPC, and (*sn*-2-$^2H_{27}$)-DMPC were purchased from Avanti Polar Lipids (Birmingham, AL) and used without further purification. D_2O and deuterium-depleted water were obtained from Eurisotop (St. Aubin, France). Possible lipid hydrolysis was checked after completion of NMR experiments by thin layer chromatography. When more than 5% lysolipids was detected, the data were not used. Research grade KCl, NaCl, $CaCl_2$, and $MgCl_2$ salts were purchased from Sigma (St. Quentin-Fallavier, France).

Sample preparation

Appropriate quantities of DMPC and DCPC with a DMPC/DCPC molar ratio, $r_{C14/C6}$, of 3.55, were poured into a centrifuge vial, and 100 μl of D_2O ionic solutions were prepared and added to the total 25 mg of lipids, hydration (v/w) was therefore $h = 80\%$. The sample was then vortexed at 2700 rpm, centrifuged at 7500 rpm for 5 min, frozen in liquid nitrogen, and warmed up in a 50°C water bath for 10 min. This cycle was repeated between 5 and 10 times until a highly viscous, transparent gel was obtained at room temperature (Raffard et al., 2000).

NMR spectroscopy

^{31}P NMR was carried out on a Bruker Avance 400 NB spectrometer. A phase-cycled Hahn-echo pulse sequence with gated broadband proton decoupling was used (Rance et al., 1983). Deuterium (D_2O) lock was used, and 128 acquisitions were recorded. ^{2}H NMR experiments were carried out on a Bruker Avance 500 WB US spectrometer. Experiments on perdeuterated *sn*-2 DMPC chains were performed using a phase-cycled quadrupolar echo sequence, and 1000 transients were acquired (Davis et al., 1976). The same phase-cycled quadrupolar echo sequence was used to record D_2O spectra; broadband proton decoupling was used, and four scans were acquired. Typical experimental parameters were as follows: spectral width of 40 kHz for ^{31}P NMR, 500 kHz for ^{2}H NMR of perdeuterated *sn*-2 chains, and 13 kHz for D_2O spectra; $\pi/2$ pulse width of 5.8 μs for ^{31}P and 2.8 μs for ^{2}H; interpulse delays of 50 μs and recycle delays of 5 s and 1 s for ^{31}P and ^{2}H, respectively. ^{31}P chemical shifts were referenced to 85% H_3PO_4 (0 ppm). Samples were placed in the field at low temperatures, and the temperature was gently increased to the highest temperature of the series. Experiments were then recorded by decreasing temperature. Samples were allowed to equilibrate at a given temperature for 30 min before the acquisition was started. For experiments on D_2O, the sample equilibration time was 1 h.

Freeze-fracture electron microscopy

Freeze-fracture experiments were performed with a Balzers vacuum chamber BAF 300 (Balzers, Liechtenstein). A small droplet of mixture was sandwiched between two copper specimen holders and was kept at the desired temperature to reach equilibrium. The environment was saturated with water to avoid evaporation. The sandwich was then frozen with liquid propane cooled with liquid nitrogen. The frozen sandwich was additionally fixed to a transport unit under liquid nitrogen and transferred to the fracture replication stage in a chamber that was then pumped down to 10^{-6} mbar at -120°C. Immediately after fracturing, replication took place by first shadowing with platinum/carbon at 45° and then with carbon deposition at 90°. The sample was allowed to warm to room temperature. Replicas were retrieved and cleaned in water and mounted on 200-mesh copper grids. Observations were made with a Jeol 2000 FX transmission electron microscope operated at 200 kV. Images were recorded using a Lhesa EMTV10S camera (Cergy-Pontoise, France) and digitized with Quantel Sapphire hardware (Newbury, UK). The Corel Photo Paint package was used for image processing. Some of the images were recorded on AGFA Scientia films and developed using standard procedures.

Data analysis and spectral simulations

Programs to simulate NMR spectra (E. J. Dufourc, unpublished) were written in FORTRAN with the Absoft ProFortran package (Rochester Hills, MI). Data handling and analyses were performed with the Microcal ORIGIN software (Northampton, MA). When the phosphorus NMR lines were well separated, a simple integration was performed using the Bruker package. Otherwise, they were simulated according to the procedure discussed above (see Introduction).

RESULTS

^{31}P NMR of DMPC-DCPC systems

The long-chain to short-chain lipid molar ratio, $r_{C14/C6}$, and the D_2O content were kept constant ($r_{C14/C6} = 3.55$ (78% mole fraction of DMPC), and hydration = 80%) for all experiments. Depending on samples, KCl, NaCl, $CaCl_2$, and $MgCl_2$ concentrations ranged from 0 to 500 mM, and the temperature was varied from 20°C to 70–80°C to cover the domain in which bicelles magnetically align (Raffard et al., 2000).

Fig. 3 shows selected spectra for a salt concentration of 100 mM. The two left columns report the phosphorus NMR data for monovalent cations K^+ and Na^+. Spectra are very similar for corresponding temperatures; i.e., at 42°C they exhibit a single sharp line at ~ -0.2 ppm, close to the isotropic chemical shift of phosphatidylcholines and the 90° edge of a single axially symmetric powder pattern at -14.6 ppm. The 0° shoulder of this powder pattern is barely observed at 30 ppm, on increasing the vertical scale, with an abnormally very weak intensity (see vertical expansion in Fig. 3). The isotropic peak reflects the presence of micelles, and the single axially symmetric powder pattern with a very weak 0° shoulder can be attributed to a bilayer phase showing a reminiscent macroscopic orientation in the magnetic field (Pott and Dufourc, 1995). Spectra in the presence of divalent cations Ca^{2+} and Mg^{2+} at this same temperature present the same isotropic peak, but two single sharp lines of ~ -11 and -15 ppm appear instead of the 90° edge of the powder pattern. Between 30°C and 39°C, ^{31}P NMR spectra in the presence of both monovalent and divalent cations display two peaks, one of them approximately three to four times more intense than the other, the area ratios varying notably with temperature and ion concentration. In the presence of KCl and NaCl their chemical shifts vary from -2.5 to -5 ppm for the small peaks and from ~ -10 to -11 ppm for the peak of higher intensity (Table 1). With divalent ions, the chemical shift of small peaks varies between ~ -2 and -9.5 ppm and that of the larger between ~ -11 and -15 ppm. For all samples, chemical shifts generally decrease in absolute value when temperature decreases, the lower-intensity peaks drifting toward 0 ppm with a steeper slope than the higher-intensity peaks, as already reported (Raffard et al., 2000). These two sharp peaks are the signatures of bicelles oriented with the normal to the bilayer perpendicular to the magnetic field (Katsaras et al., 1997; Prosser et al., 1996). At 27°C almost all spectra display similar features, that is, broad asymmetric lines near -1 ppm and regular axially symmetric powder patterns with 90° edges around -9 to -10 ppm and 0° shoulders near 19 ppm. The spectrum in the presence of $CaCl_2$ at 27°C deserves a special comment. Peaks are sharper than in the presence of other ions and have chemical shift values of -12.2, -1.9, and -0.2 ppm. The 0° shoulder is barely detected. Regular axially symmetric powder patterns detected in the presence of K^+, Na^+, and Mg^{2+} reflect the character of macroscopically nonoriented material. The features observed in the presence of Ca^{2+} at 27°C clearly indicate the presence of oriented bicelles. For lower temperatures, spectra show a powder pattern together with a broad isotropic line, for all studied cations. Below 20°C, all the systems show spectra composed of a single isotropic line characteristic of small tumbling objects (not shown). ^{31}P NMR spectra of lipid mixtures with 100 mM $CaCl_2$ and $MgCl_2$ were recorded at higher temperatures. Above 42°C and up to 60°C, spectra displayed an isotropic peak centered at ~ -0.2 ppm and a dominant peak at ~ -15 ppm. A small peak at ~ -14 ppm systematically appeared merged into this intense peak. Interestingly, the intensity of the isotropic line at -0.2 ppm increased up to temperatures near 45–50°C and then decreased upon increasing further the temperature. It almost disappeared for temperatures near 70–80°C (not shown).

Fig. 4 presents the ^{31}P NMR spectra of the lipid mixtures at 36°C, i.e., well within the domain where bicelles align in the field, with varying NaCl concentration. In the absence of salt (left spectrum), the two NMR lines characteristic of bicelles are resolved but exhibit very asymmetric shapes with detectable intensity up to 10 ppm. This behavior could be simulated by a Gaussian distribution of bicelle orientations with $\eta = 17° \pm 2°$ as described in Theoretical Background and as shown in Fig. 2. Here it must be mentioned that the homogeneous broadening ($\sim$50 Hz) was estimated with a Hahn echo se-

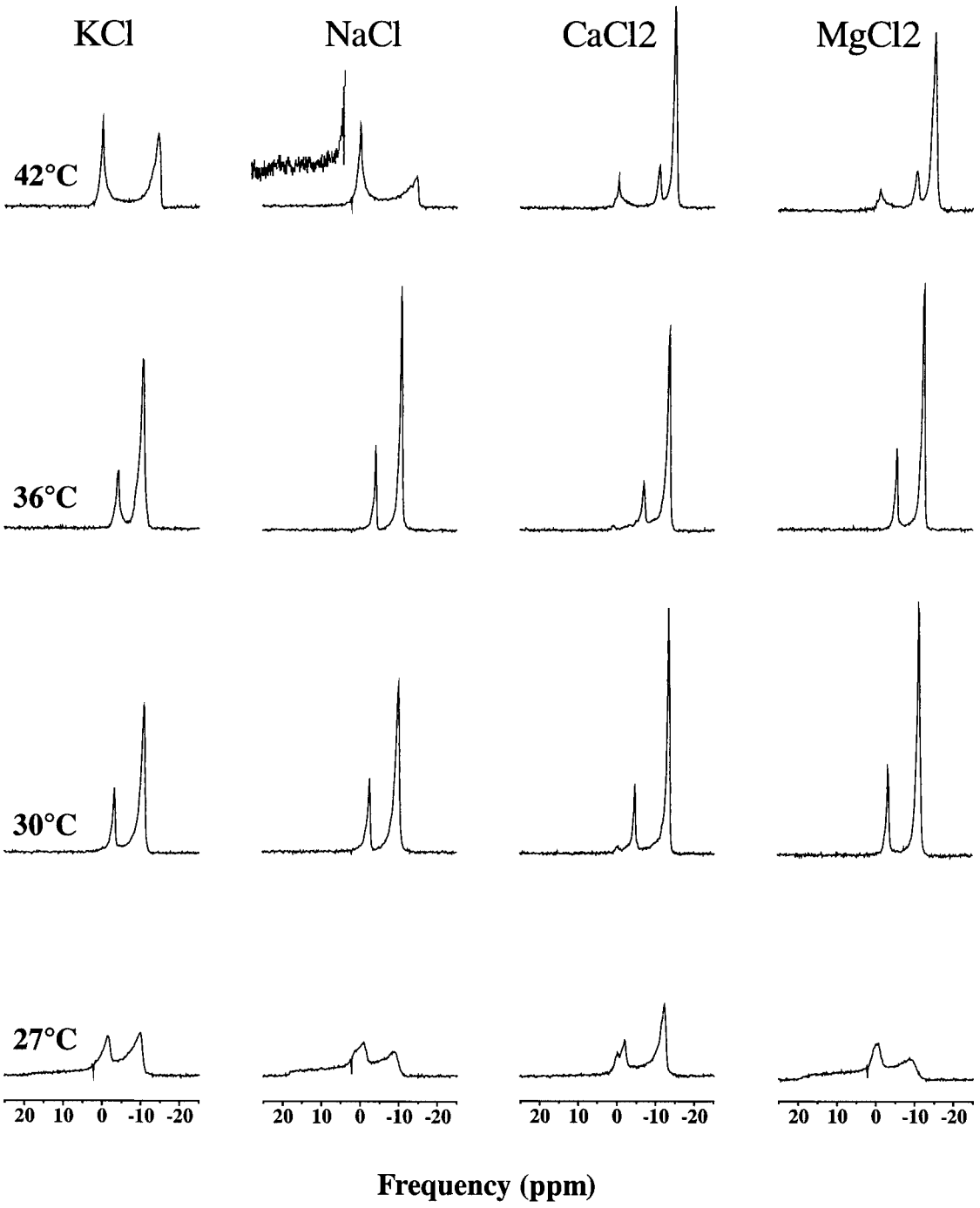

FIGURE 3 Proton-decoupled ^{31}P NMR spectra of DMPC and DHPC mixtures in 80% (w/v) D_2O in the presence of 100 mM KCl, NaCl, $CaCl_2$, and $MgCl_2$. Mole fraction, X = [DMPC]/([DMPC] + [DHPC]), is 78%, and temperature is indicated on the spectra. One thousand transients were acquired with the Hahn echo pulse sequence under deuterium lock conditions, and 10-Hz line broadening was applied before Fourier transformation. Chemical shifts are expressed relative to 85% H_3PO_4 (0 ppm). Spectra are plotted in absolute vertical scale.

quence and used to simulate spectra. The Gaussian distribution of orientations used for simulations leads in fact to an inhomogeneous broadening resulting in an apparent width at half-maximum of ~300 Hz. In the presence of increasing concentrations of NaCl, the lines sharpen. They become almost symmetrical for a concentration of 100 mM. This could be simulated with a mosaic spread of 6° ± 2°. At 200 mM NaCl, they broaden again and become asymmetrical. The calculated mosaic spread is then of the order of 10°. Similar experiments were repeated with the other salts, and concentrations of [KCl] = 200 mM, [$CaCl_2$] = 50 mM, and [$MgCl_2$] = 100 mM yielded the sharpest peaks.

TABLE 1 ^{31}P NMR chemical shifts of DMPC/DCPC in the presence of 100 mM salts

Temperature (°C)	No salt	KCL	NaCl	$CaCl_2$	$MgCl_2$
27	−10.6, −1.9	−9.9, −1.6	−9.0, −1.0	−12.2, −1.9, −0.2	−8.7, −0.7
30	−11.2, −3.5	−11.0, −3.3	−10.1, −2.6	−13.4, −4.7	−11.3, −3.3
33	−11.5, −4.4	−10.4, −3.5	−10.6, −3.5	−13.6, −6.9	−12.2, −4.5
36	−11.8, −5.4	−10.7, −4.4	−10.9, −4.2	−14.0, −6.9	−12.7, −5.6
39	−14.3, −9.5, −3.9	−14.2, −9.0, −3.8	−11.0, −5.0	−15.1, −9.5, −0.4	−13.0, −6.6
42	−14.6, −0.1	−14.5, −0.2	−14.8, −0.2	−15.1, −11.0, −0.4	−15.6, −10.8, −1.3

Accuracy is ±0.2 ppm. Chemical shifts are expressed relative to 85% H_3PO_4 (0 ppm).

Within the region where bicelles align in the field, the area of the two NMR lines was determined either by simple integration or by spectral simulation when there were superposition of signals due to the long tailing of bands. The q factor was then calculated and reported in Table 2. For a given ion concentration, it was found to be the same, within the experimental error, for four to six measurement temperatures spanning the range 27–40°C. Therefore we report q values as the average over these four to six measurements (Table 2). It is noticeable that q values markedly differ from the initial long-chain versus short-chain ratio used for sample preparation ($r_{C14/C6} = 3.55$).

^{2}H NMR of DMPC *sn*-2 chains

Solid-state deuterium NMR experiments were performed on similar lipid mixtures using DMPC perdeuterated on the *sn*-2 chain and H_2O instead of D_2O. Salt concentrations were 100 mM, and temperatures ranged from 25°C to 66°C.

Fig. 5 displays ^{2}H NMR spectra for selected temperatures, in the presence of NaCl, $CaCl_2$, and $MgCl_2$. At 25°C, an isotropic line superimposed on a powder pattern is observed that depicts the presence of an isotropic phase with nonoriented bilayers. This is in agreement with correspond-

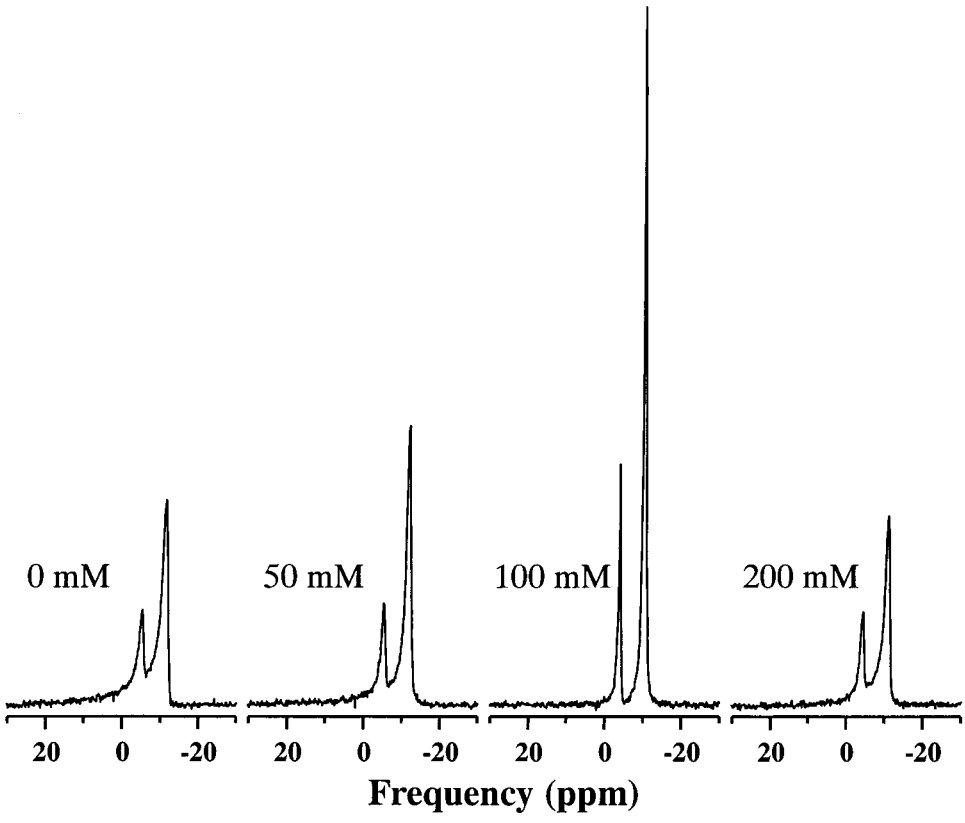

FIGURE 4 Proton-decoupled ^{31}P NMR spectra of DMPC and DHPC mixtures in 80% (w/v) D_2O in the presence of various concentrations of NaCl. Mole fraction, X = [DMPC]/([DMPC] + [DHPC]), is 78%, and temperature was set to 36°C. One thousand transients were acquired with the Hahn echo pulse sequence under deuterium lock conditions, and 10-Hz line broadening was applied before Fourier transformation. Chemical shifts are expressed relative to 85% H_3PO_4 (0 ppm). Spectra are plotted in absolute vertical scale.

TABLE 2 Bicelles sizes as found from ^{31}P NMR and freeze-fracture electron microscopy

Concentration (mM)	KCl		NaCl		$CaCl_2$		$MgCl_2$	
	q*	Φ_{NMR}†	q	Φ_{NMR}	q	Φ_{NMR}	q	Φ_{NMR}
0	2.58	370	2.58	370	2.58	370	2.58	370
50	2.70	380	2.77	390	4.24	570	3.36	460
100	2.63	**370**	2.79	**390**	4.33	**580**	3.34	**460**
150	ND	ND	2.89	410	3.53	480	3.97	530
200	2.58	370	2.67	380	3.64	500	4.17	560
	$W_{1/2}$‡	Φ_{FFEM}§	$W_{1/2}$	Φ_{FFEM}	$W_{1/2}$	Φ_{FFEM}	$W_{1/2}$	Φ_{FFEM}
100	65	**310**	50	**250**	140	**510**	70	**450**

ND, not done.

*Area of peak at ~−11 ppm over area of peak at ~−4 ppm. Figures are the average over four to six values for temperatures within the domain of bicelle alignment (27–40°C). Accuracy is 10%.

†Bicelle diameter according to Eq. 5 of text. Accuracy is 10%.

‡Half-width at half-maximum of Gaussian function used to fit data of Fig. 8.

§Bicelle mean size from Gaussian fit of Fig. 8 data.

ing ^{31}P NMR spectra (vide supra). Spectra at 36°C show a typical pattern of chain-perdeuterated DMPC molecules with their long axis oriented perpendicular to the magnetic field. Note that at 36°C, i.e., well within the domain in which bicelles align, up to 11 quadrupolar splittings are detected with a remarkable resolution. Even the quadrupolar splittings for positions 2R and 2S are detected at ±5.5 and ±7 kHz with, of course, a lower intensity (Engel and Cowburn, 1981). Very small quadrupolar splittings that are also detected near 0 Hz can be assigned to deuterium natural abundance of water because the sample was not prepared with deuterium-depleted water (vide infra). Between 42°C and 54°C, the chain splittings are still detected, but with a lesser resolution, and the isotropic signal near 0 Hz increases with temperature. For divalent cations, this isotropic line starts to decrease for temperatures >60°C, in agreement with the ^{31}P NMR observation. It is remarkable that at 66°C the quadrupolar splittings are very well resolved and that the spectrum exhibits characteristics of a sample for which most of the material is macroscopically oriented in the magnetic field. The quadrupolar splittings, $\Delta\nu_Q$, were measured at 36°C and 60°C, and the corresponding S^{CD} order parameters were calculated using the following equation: $S^{CD} = 4\Delta\nu_Q/3A_Q$, where $A_Q = 167$ kHz is the quadrupolar coupling constant for methylene bonds (Burnett and Müller, 1971). Values are reported in Table 3, together with corresponding data on extended bilayers (pure DMPC liposomes in L_α phase) from Douliez et al. (1995) and with order parameters from DMPC-DCPC bicelles in the presence of 100 mM KCl ($X = 75\%$; $h = 80\%$ (Raffard et al., 2000)) for comparison. Attribution and sign determination was made on the basis of extended bilayers. For a given temperature, it is remarkable that all chain order parameters, in the presence of Na^+, Ca^{2+}, and Mg^{2+} are the same, within 2.10^{-3}, independently of the cation added. Order parameters with $X = 78\%$ are generally smaller than for pure DMPC liposomes ($X = 100\%$) but greater than for bicelles with $X = 75\%$. The average chain length, $\langle L\rangle$, was calculated from these data according to Douliez et al. (1995, 1996) and also reported in Table 3. The accuracy of such a calculation is of the order of 0.1 Å because the accuracy in quadrupolar splitting measurement is very high (~10 Hz). It can be remarked that the chain length of DMPC in bicelles is shorter by 0.6 Å compared with that in 100% DMPC liposomes, for the same temperature. A small variation in the DCPC content ($X = 78\%$ vs. $X = 75\%$) in the bicelle, although markedly modifying the individual chain order parameters, does not modify the chain length, within 0.1 Å. The bilayer thickness, $2a$, may be estimated by combining NMR, x-rays, and neutron and molecular mechanics simulations (Büldt et al., 1979; Douliez et al., 1996; Hauser et al., 1981; Léonard et al., 2001): $2a = 2\langle L\rangle + 16 \pm 1.0$ Å. This leads to $2a = 38 \pm 1.0$ Å for the bicelles of our present study. The bicelle diameter, Φ_{NMR}, as given by Eq. 4, may then be calculated on the basis of NMR data. The corresponding values are reported in Table 2.

^{2}H NMR of D_2O

Water structure and dynamics were probed by D_2O in samples with 100 mM salt concentration. ^{2}H NMR spectra were recorded from 24°C to 66°C for monovalent cations and up to 84°C for divalent cations. It must be mentioned that a marked hysteresis was obtained during the first temperature run. It was therefore necessary to wait 1 h at a given temperature to obtain reproducible data. Spectra for selected temperatures are shown in Fig. 6. At 24°C and below, an isotropic line is detected in accordance with ^{31}P NMR data. A unique quadrupolar splitting is detected from 27°C to 42°C. This also agrees with the appearance of magnetically aligned bicelles as detected from the lipid viewpoint (vide supra). Interestingly, the splitting is about the same independently of cations. For $T \geq 48$°C, the water spectrum is composed of an isotropic line superimposed on a quadrupolar splitting. However, there is a strong difference between monovalent and divalent cations: 1) the isotropic line that coexists with the quadrupolar doublet tends to disappear with increasing temperature above 60°C (especially in the presence of Ca^{2+}), and 2) the quadrupolar splitting is about constant between 48°C and 84°C with a plateau value two to three times greater for monovalent than for divalent cations. The thermal evolution of both the chemical shift and the quadrupolar splitting is reported in Table 4. The chemical shift was arbitrarily set to zero at 24°C where a single isotropic sharp line is observed. When the spectrum is composed of a single quadrupolar splitting, the chemical shift is measured as the doublet center. For $T \geq 48$°C, the chemical shift measured on the isotropic line does not correspond to the center of the quadrupolar splitting also detected. Hence two figures are given in Table 4, and the one in italics reports the direct

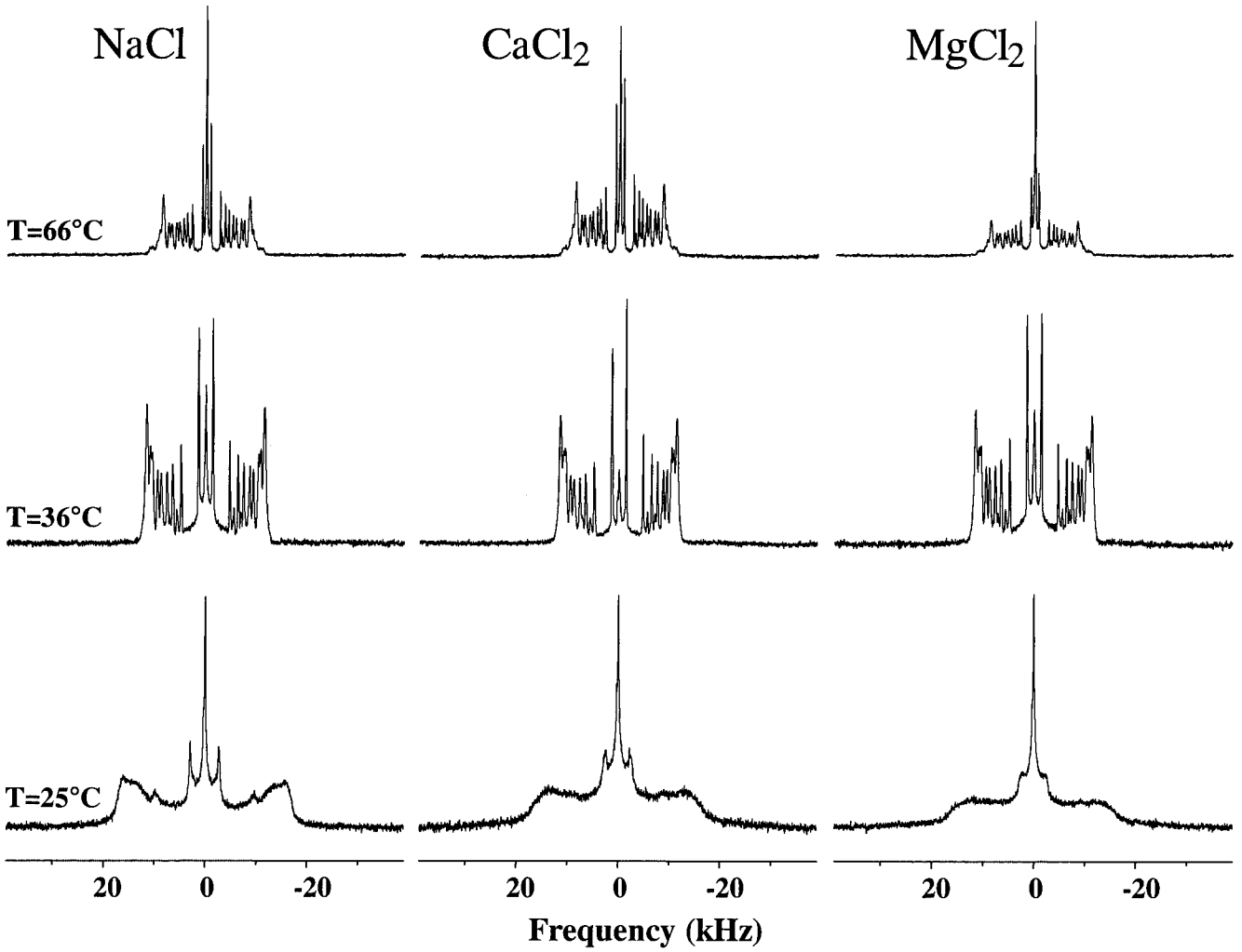

FIGURE 5 Temperature dependence of ^{2}H NMR spectra of *sn*-2 perdeuterated DMPC embedded in a DMPC/DCPC system (X = 78%; 80% H_2O) in the presence of 100 mM NaCl, $CaCl_2$, or $MgCl_2$. Temperature is 25°C (*bottom*), 36°C (*middle*), and 66°C (*top*). NMR signals were acquired with the quadrupolar echo pulse sequence. One thousand acquisitions were collected, and a line broadening of 20 Hz was applied before Fourier transformation. The isotropic line was arbitrarily set to 0 Hz.

measurement on the isotropic line. As a global observation, the temperature variation of the chemical shift of isotropic lines and doublet from 27°C to 42°C roughly fits on a linear regression. It may be noted that the slopes are slightly different from cation to cation.

Freeze-fracture electron microscopy

Samples with $X = 78\%$ and $h = 80\%$ were also prepared in the presence of 100 mM of KCl, NaCl, $CaCl_2$, and $MgCl_2$. Representative images are shown in Fig. 7 for the four cations used, where more or less discoidal objects are observed. For images taken with NaCl and KCl (Fig. 7, *A* and *C*), diameters of these disk-like objects are smaller than in the images taken with $CaCl_2$ and $MgCl_2$. For each of the samples, the longest dimension of 100–150 anisotropic objects was measured and a size histogram built using a step size of 40–50 Å. Fig. 8 shows the corresponding histograms for bicelles in the presence of the four cations. The distributions show a reasonable monodispersity although displaying some asymmetrical shape that may be accounted for by the way the object size was measured. Although the distributions do not resemble a trivial function, they were fitted by a Gaussian (solid bold line) to characterize the mean size and the width of the distribution. Results are reported in Table 2. It clearly appears that in the presence of monovalent cations the object mean size is on the order of ~300 Å with a half-width on the order of 50 Å. With calcium and magnesium, objects have a mean size of ~500 Å. The width of the distribution observed in the presence of $CaCl_2$ (140 Å) is at least twice that observed for other cations.

TABLE 3 DMPC order parameters as a function of labeled carbon position

k*	36°C†	60°C†	Liposomes‡	$X = 75\%$§
2	0.089	0.055	0.094	0.070
2	−0.113	−0.070	−0.141	−0.103
3	−0.172	−0.126	−0.212	−0.157
4	−0.182	−0.143	−0.220	−0.167
5	−0.182	−0.143	−0.220	−0.167
6	−0.182	−0.143	−0.222	−0.167
7	−0.182	−0.143	−0.216	−0.167
8	−0.166	−0.117	−0.210	−0.157
9	−0.151	−0.101	−0.198	−0.157
10	−0.139	−0.093	−0.176	−0.143
11	−0.121	−0.076	−0.161	−0.131
12	−0.103	−0.065	−0.139	−0.110
13	−0.076	−0.048	−0.111	−0.088
14	−0.022	−0.014	−0.027	−0.021
$\langle L \rangle$¶	10.9	10.4	11.5	10.9

*Labeled carbon position.

†S_{CD} values for DMPC in bicelles (78% DMPC; 80% hydration) at 36°C and 60°C in the presence of 100 mM $CaCl_2$, $MgCl_2$, and NaCl. Figures for the three salts are the same within 2×10^{-3}, so only one column is reported.

‡DMPC as water dispersion (large multilamellar vesicles). Data are from DMPC labeled on the *sn*-2 chain, from Douliez et al. (1995), at 35°C.

§DMPC in DMPC-DCPC bicelles (75% DMPC, 80% hydration, 100 mM KCl, and 35°C) from Raffard et al. (2000).

¶Average chain length (see text) in Å; accuracy, ±0.1 Å.

DISCUSSION

Several findings have been presented. 1) Solid-state NMR can be used in a quantitative manner to measure cation-induced modulation of bicelle size and magnetic alignment in the field. 2) For the first time, freeze-fracture electron micrograph images of bicelles allowed us to measure the dimensions of these bicelles, and the measurements are in agreement with those made with NMR. 3) The temperature domain of existence of magnetically aligned bicelles is slightly increased in the presence of divalent cations. 4) All investigated cations promote better macroscopic bicelle orientation in the magnetic field. And 5) the bicelle dynamics in the bilayer core remains mainly unchanged, whereas different hydration effects are promoted by monovalent and divalent cations. These findings will be sequentially discussed below.

Size of bicellar disks

Bicelle diameters have been determined by two very independent techniques. On one hand, solid-state NMR data, by simple integration of the ^{31}P NMR peaks, allows bicelle diameter calculation by means of Eq. 5. This measurement is based on a model describing the bicelle as a disk made of long-chain lipids surrounded by half a torus of short-chain lipids and leads to bicelle diameters of ~380 Å with monovalent cations, 460 Å with Mg^{2+}, and 580 Å with Ca^{2+} (see Table 2, 100 mM). On the other hand, freeze-fracture electron microscopy directly gives the mean size and distribution and is in principle model-free. Electron microscopy images clearly show that the currently admitted description of a bicelle under the form of a discoidal object is totally justified in the temperature-composition-hydration domain of this study. The bicelle diameters obtained from electron microscopy images, in the presence of monovalent species, are ~300 Å with a quite low polydispersity (~20%) showing 20–50% underestimation compared with NMR determination. With divalent cations, the diameter is ~500 Å with a polydispersity ranging from 15% to 27%, and the difference with NMR measurements drops down to 0–14%, i.e., within experimental error. Considering that these data were obtained independently from two techniques, they do show quite good agreement and also indicate that the model sketched in Fig. 1 is generally valid. Artifacts inherent to two techniques may cause the discrepancy observed with monovalent salts. First, it may come from a violation of the flat disk-torus geometry that may lead NMR to overestimate the bicelle diameter. Such a violation might occur if the bicelle shape is not exactly a flat disk. For example, it could bulge in its center or with a rougher surface with some undulations. Another possible cause of discrepancy could be that the bicelles are not exactly round but have some oval shape with monovalent salts. Because we measure the longest dimension on the electron microscopy images, this might cause some size misestimation.

It is interesting here to compare our data with recent work. On one hand, Nieh and coworkers report SANS data at 10°C and 45°C on a system similar to ours ($X = 76\%$; $h = 80$–98%; 1% Tm^{3+}) and sketched a phase diagram that suggests that disks exist only at and below 25°C (Nieh et al., 2001). They favor a perforated lamellar phase above 35°C, in apparent contradiction with our data. Gaemers and Bax (2001), measuring the diffusion of a tracer in the water medium of bicelle systems for $T = 10$–35°C and $h = 90$–95%, tend also to favor that model. On the other hand, Gawrisch and colleagues, working with solid-state deuterium NMR and proton MAS on a lipid mixture with $X = 81\%$ and $h = 75\%$, report a phase that magnetically orients between 32°C and 36°C. In these conditions, they report no magnetization exchange between DMPC and DCPC, confirming that both lipids experience limited physical contact (Sternin et al., 2001). However, the authors were unable to distinguish between disks and perforated bilayers. The SANS data did not really investigate the temperature range (30–40°C) where we clearly visualize the disks by electron microscopy. In addition, we have previously shown that for a sample containing 75% DMPC, which forms magnetically orientable disks between 30°C and 40°C ($h = 80\%$), the temperature domain shrinks to 1°C upon dilution ($h = 95\%$) (Raffard et al., 2000). This may cause problems for SANS data in dilution experiments, and the diffusion experiments of Gaemers et al. might have been performed near a phase boundary region. The temperature range reported by Gawrisch and colleagues for the bicelle phase appears to be

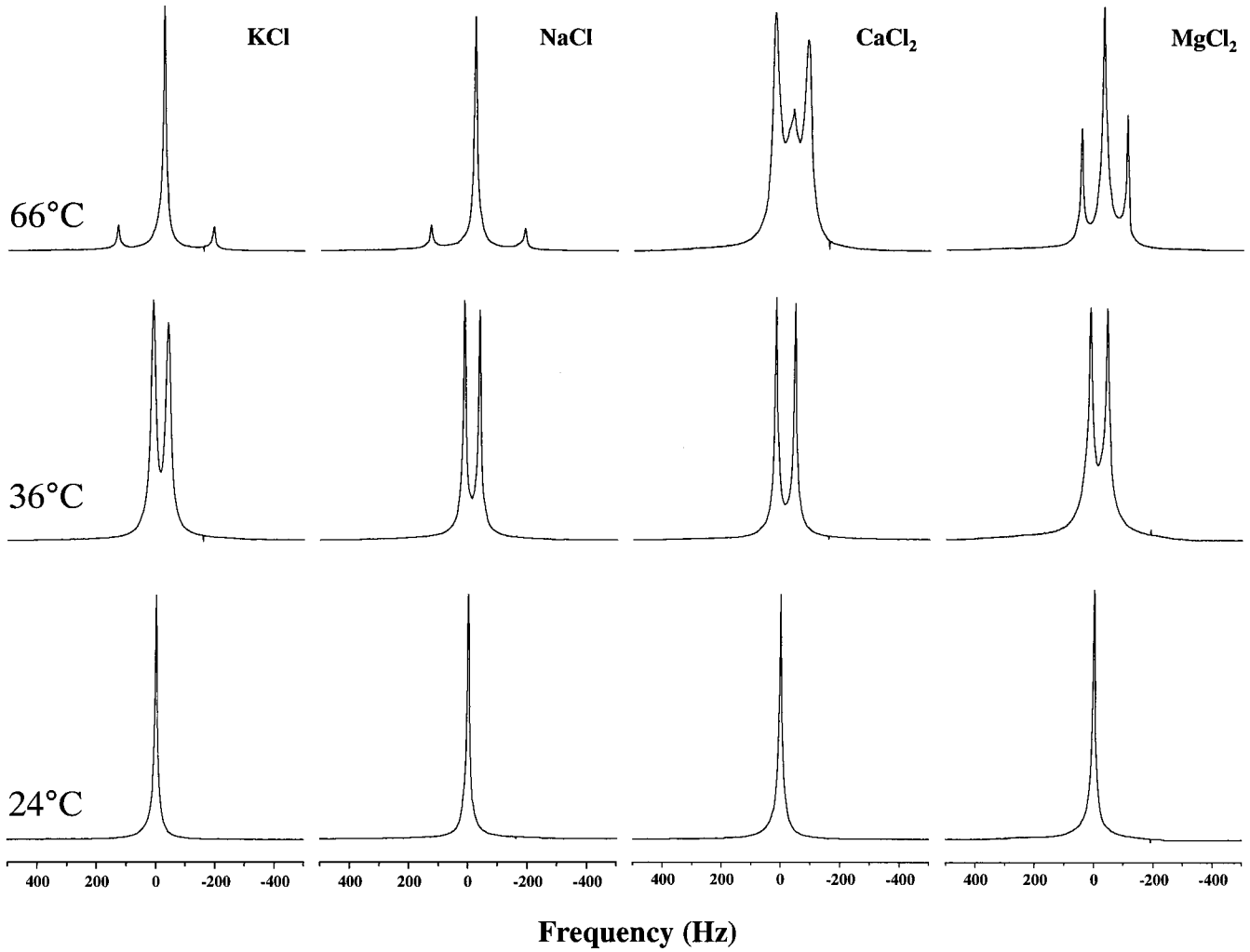

FIGURE 6 Temperature dependence of ^{2}H NMR spectra of D_2O in a DMPC/DCPC system (X = 78%; 80% D_2O) in the presence of 100 mM KCl, NaCl, $CaCl_2$, and $MgCl_2$. Temperature is indicated on the spectra. NMR signals were acquired with the quadrupolar echo pulse sequence, and 128 acquisitions were collected. The frequency axis was referenced by setting the isotropic line observed at 24°C to 0 Hz.

smaller than ours. Again, our previously published temperature-composition diagram can easily account for this. The magnetically orientable bicellar phase has an ovoid shape with boundaries close to X = 87% and 65%. For these limiting cases, the temperature range for bicelle alignment is very small (~1–3°C), the maximum range being attained for X = 78–75%. Their data are in complete agreement with ours, the X = 78% composition of the present study affording a greater temperature span.

Domain for bicelle magnetic alignment

Both ^{31}P and ^{2}H NMR of lipids indicates clearly that for all four cations studied, the temperature domain where bicelles (X = 78%; h = 80%) align in the magnetic field roughly ranges from 30°C to 40°C. As discussed above, this composition ensures the widest temperature span for bicelle alignment. When heating above 40°C, the system clearly transforms into two phases: mixed micelle (DCPC-rich) and extended bilayers (DMPC-rich) that are still macroscopically oriented (bilayer normal perpendicular to the field) (Raffard et al., 2000; Sternin et al., 2001). It is noteworthy that macroscopic orientation outside the bicelle domain is observed only when the system is heated from the bicelle state. Bringing the sample directly from low to high temperatures, outside the magnetic field, shows the two above described phases without orientation effects. This is puzzling and clearly deserves more investigation. Based on our experiments that lasted several hours at high temperatures ($T > 50$°C), we cannot say whether the thermodynamically stable state is the unaligned or aligned one. It must be noted that these two phases may be macroscopically separated by centrifugation (T. Labrot, E. J. Dufourc, and R. Oda, in preparation). For monovalent cations, this phase separation

TABLE 4 D_2O quadrupolar splittings and chemical shifts in DMPC/DCPC samples in the presence of 100 mM salts

Temperature (°C)	KCL		NaCl		$CaCl_2$		$MgCl_2$	
	δ	$\Delta\nu_Q$†	δ	$\Delta\nu_Q$	δ	$\Delta\nu_Q$	δ	$\Delta\nu_Q$
24	0	0	0	0	0	0	0	0
27	−2	5	−2	6	−2	0	−2	0
30	−6	24	−4	24	−5	16	−4	20
33	−8	36	−7	38	−8	44	−8	45
36	−10	42	−9	43	−10	50	−9	48
39	−12	46	−10	47	−13	56	−11	52
42	−14	50	−13	51	−13	63	−13	57
48	−23, *−16*	296	−20, *−14*	296	−19, *−16*	99	−17	66
54	−27, *−21*	326	−25, *−18*	323	−22, *−21*	123	−24, *−20*	160
60	−31, *−24*	323	−29, *−21*	318	−26, *−24*	123	*−27*, *−24*	162
66	−33, *−27*	326			−33, (*−34*)	110	−31, *−28*	156
72					−35	107	−35, *−33*	151
78					−40	103	−39, *−36*	150
84					−43	104	−41, *−43*	151

*Chemical shift expressed in hertz (76.8 Hz = 1 ppm). When a quadrupolar splitting is detected, the chemical shift is measured as the doublet center. Figures in italics report the chemical shift as directly measured on an isotropic line that is not coincident with the doublet center. Chemical shift was arbitrarily set to 0 at 24°C. Accuracy is ±2 Hz.

†Quadrupolar splitting; accuracy is ±2 Hz.

readily occurs at 42°C, whereas for divalent cations the NMR shows that the domain for bicelle alignment is extended to higher temperatures. In addition, the mixed micelles tend to disappear for high temperatures, especially in the presence of Ca^{2+}. NMR data also show that the lower temperature limit of magnetically aligned bicelles is 30°C for K^+, Na^+, and Mg^{2+}, whereas it is slightly lower for Ca^{2+}, 27°C. Below such temperatures, the phosphorus spectra suggest that bicelles still exist but do not orient in the magnetic field. However, the nature of the system in such conditions is not well understood. NMR shows the coexistence of two very different spectral features (broad isotropic line and powder pattern), whereas no macroscopic separation was observed. They might reflect the progressive bicelle formation from the isotropic phase detected below 24°C. To summarize, for monovalent cations K^+ and Na^+, the whole system is under the form of aligned bicelles on an ~10°C temperature range, and this range appears to be slightly extended for divalent cations.

Modulation of bicelle alignment by cations

The presence of cations has a dramatic effect on bicellar alignment with the magnetic field as can be observed from the ^{31}P NMR spectra. The broad and asymmetric peaks of ~300-Hz line width at half-maximum in the absence of salts get thinner (~90 Hz), much more intense, and almost symmetrical with salts as can be seen in Fig. 4. Because the homogeneous broadening may be estimated to be 50 Hz, a Gaussian distribution of bicelle orientations ranging from 17° without salts to 6° with salts at best alignment can quantify the inhomogeneous broadening. This mosaic spread is comparable to that obtained by neutron diffraction on a similar bicelle sample containing Tm^{3+} (Katsaras et al., 1997). For each of the four salts investigated, there is an optimum salt concentration for best alignment. It ranges from 50 mM with $CaCl_2$ to 200 mM with KCl. There is no straightforward relationship between the ion charge and the concentration at which the best orientation is observed. This may be related to the fact that possible traces of salts may already be present in commercial lipids.

Losonczi and Prestegard (1998) already observed such an increase in macroscopic alignment when bicelles are doped with cetyltrimethylamonium bromide. It was accounted for by invoking a delicate balance between van der Waals and electrostatic forces between bicelles that might, for certain ion concentrations, lead to a secondary minimum when considering the potential energy of interaction of bicelles as a function of inter-object distance. In other words, macroscopic orientation will pass by a maximum as a function of ionic concentration; this is indeed what we observe (vide supra). It is also interesting to consider the orientation phenomenon from the molecular point of view. As shown in the pioneering work of Helfrich and coworkers (Boroske and Helfrich 1978; Scholz et al., 1984) on the magnetic anisotropy of membranes, bilayer annealing is primarily caused by the negative $\Delta\chi$ of phospholipids. The fact that all investigated cations contribute to a better bicelle self-orientation seems to show an increase in the phospholipid $\Delta\chi$ absolute value. Unfortunately, there are few data on the effect of cations on the magnetic susceptibility, and magnetic anisotropy measurements on phospholipid membranes in the presence of our cations are clearly needed.

Water and DMPC chains dynamics in bicelles

Within the domain where bicelles align in the field, the lipid hydrocarbon chains experience the same order parameters,

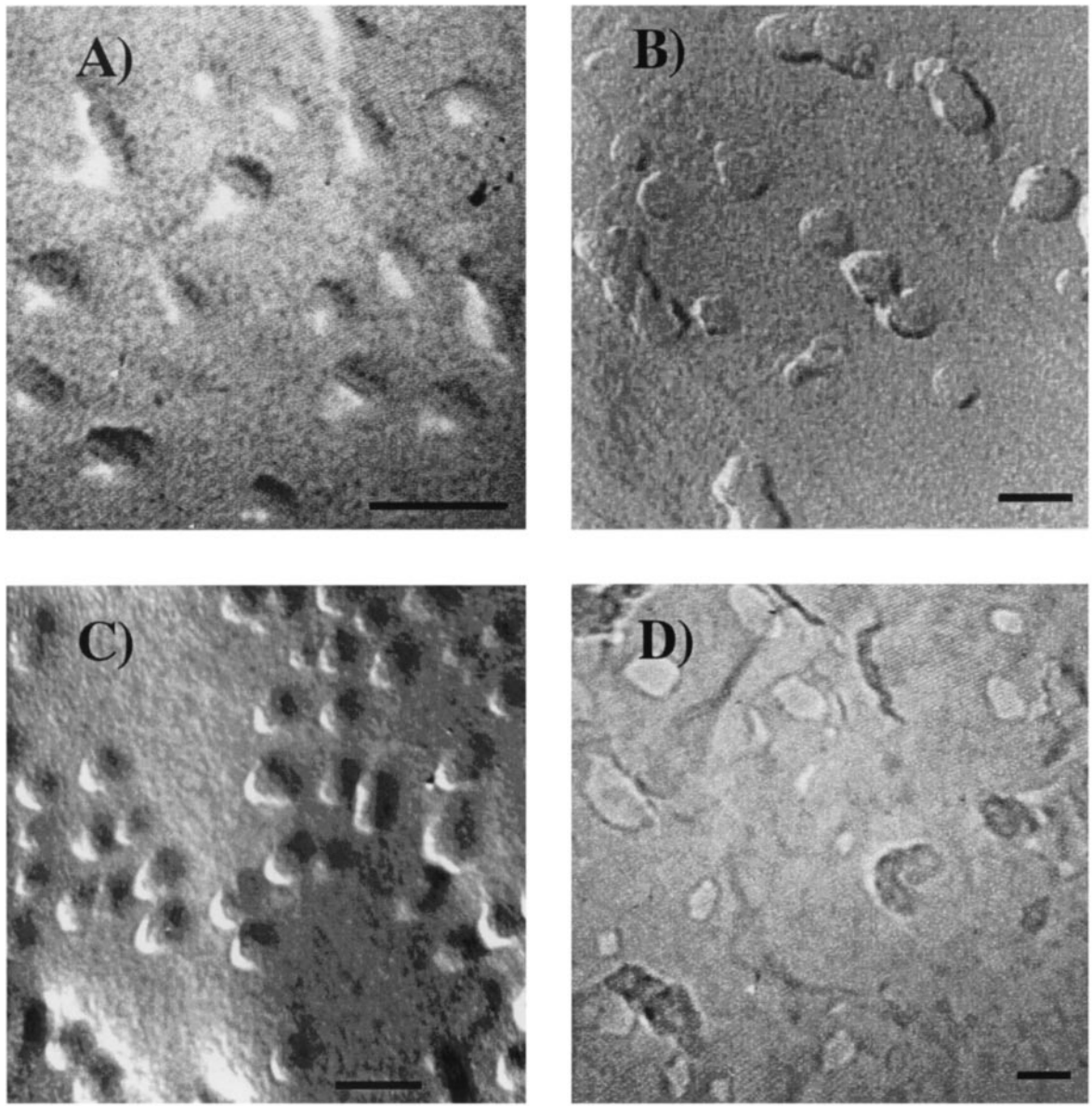

FIGURE 7 Freeze-fracture electron microscopy pictures of DMPC/DCPC systems (X = 78%; 80% H_2O) in the presence of 100 mM NaCl (*A*), $CaCl_2$ (*B*), KCl (*C*), and $MgCl_2$ (*D*). Samples were frozen from 35°C, a temperature for which all systems are in the domain of bicelle magnetic alignment (27–40°C). The bar in each of the pictures measures 50 nm.

independently of cation nature. Bridging effects at the headgroup level that are suspected to occur in the presence of divalent cations do not modify the hydrophobic bilayer thickness, hence showing that the chain behavior is disconnected from the headgroup dynamics. At 60°C, i.e., outside the bicelle domain, the chain length is of 10.4 Å, compared with 10.7 Å that was observed with pure DMPC (Douliez et al., 1996). This indicates that the DMPC-rich bilayers perceive the disordering effect of some DCPC molecules.

The effect of temperature on water dynamics is quite interesting. For all cations, a quadrupolar splitting increasing from 0 to ~50–60 Hz is observed in the domain where bicelles align. As already described by Raffard et al. (2000), it is the result of a two-site exchange between water located at the bicelle surface and water further away that swells the system. The peculiar line shapes that are observed clearly indicate that the rate of exchange is in the range fast to intermediate. Because there are ~10 water molecules tightly bound per phosphatidylcholine headgroup (Faure et al., 1997), the residual quadrupolar splitting is very small at 80% hydration (water-to-lipid ratio of ~130): the majority (92%) of water molecules undergo isotropic tumbling and exchange with the small fraction of bound anisotropic water. Assuming that one can extend data obtained on lipo-

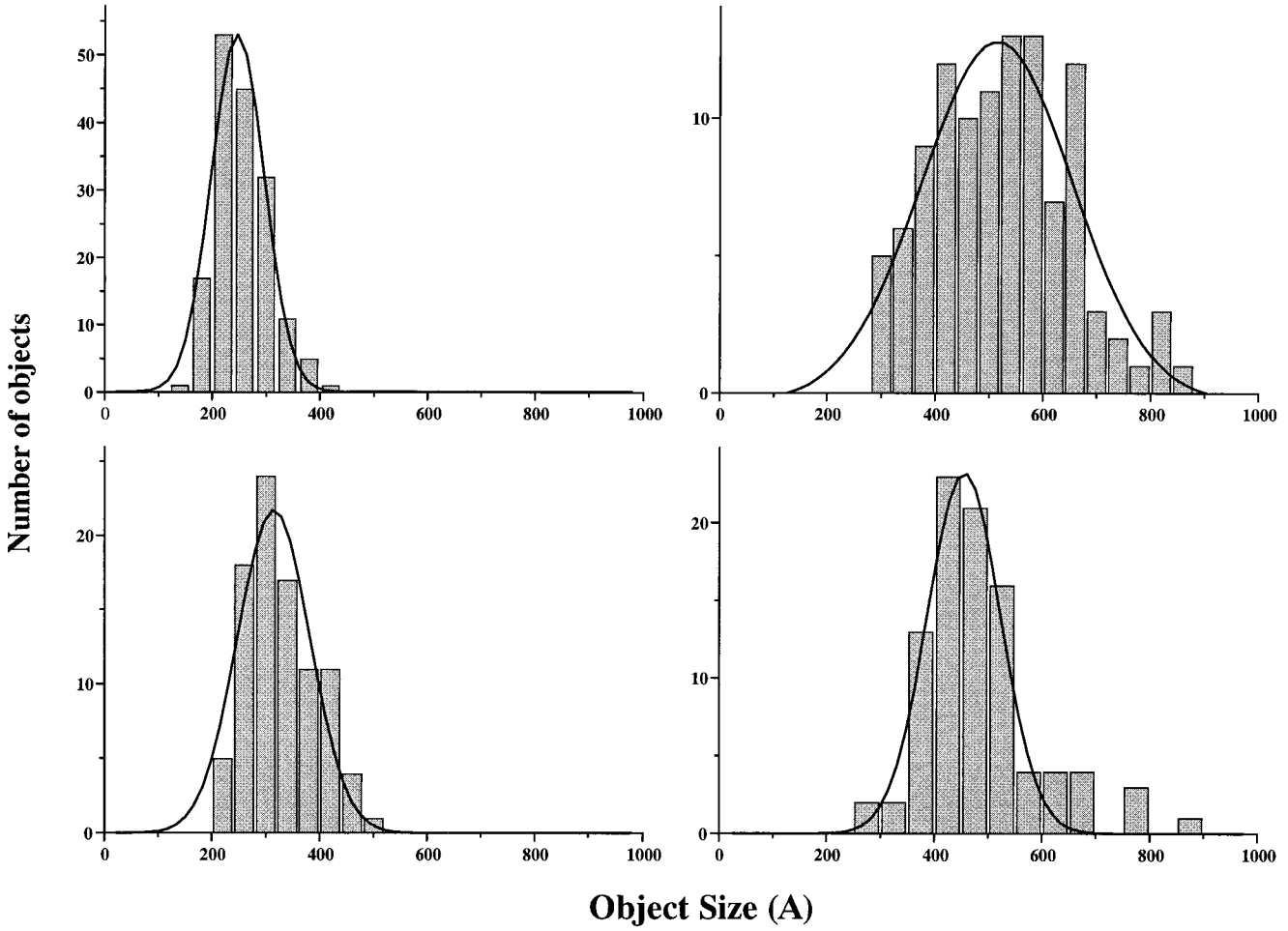

FIGURE 8 Histograms of size distribution for DMPC/DCPC systems (X = 78%; 80% H_2O), in the presence of 100 mM KCl, NaCl, $CaCl_2$, and $MgCl_2$. Objects were measured on the electron micrograph pictures (Fig. 8). Histograms were built with a frequency count for object size of 40–50 Å and analyzed by a Gaussian function (*solid bold line*).

somes (1200 Hz for the quadrupolar splitting of 10 bound water molecules per lipid (Faure et al., 1997)) to bicelles, a quick calculation predicts 90 Hz for the residual quadrupolar splitting in bicelles at 80% hydration. We observe values on the same order of magnitude, indicating that the above model for water dynamics is reasonable for bicelles. Of interest is nonetheless the fact that all the water molecules, on average, are ordered. NMR has already used this fact for protein structure determination where soluble proteins are dissolved in the water of the bicelle phase: a residual dipolar ordering can thus be measured and used for distance restraints.

The water dynamics is quite different for temperatures on each side of the above range. Isotropic lines that are observed at temperatures below the domain for bicelle alignment are indicative of water in isotropic environment (small aggregates/mixed micelles and bulk solution). For temperatures above the domain of bicelle magnetic alignment, the water spectrum is composed of an isotropic line plus a quadrupolar splitting. This is indicative of a slow exchange, on the NMR time scale, between isotropic and anisotropic water. Again, the peculiar line shapes are indicative of an exchange regime coming close to intermediate. At these temperatures, the system contains DMPC-rich bilayers and DCPC-rich micelles (T. Labrot, E. J. Dufourc, and R. Oda, in preparation; Raffard et al., 2000). The isotropic line is therefore assigned to water interacting with micelles and the quadrupolar splitting to water exchanging with the bilayer surface. As monitored by the isotropic chemical shift (Table 4), the water electronic environment is slightly different in a micelle-type environment than in a lamellar-type one. It is interesting to note that water dynamics in this upper temperature biphasic domain is very different in the presence of monovalent versus divalent cations. A quadrupolar splitting of ~300 Hz is observed for K^+ and Na^+. It drops down to ~100–150 Hz in the presence of Ca^{2+} and Mg^{2+}. It is difficult to extract water dynamics from these data because the two-site exchange model is no longer valid in this

two-phase domain. We can only note that the different behavior already pointed out for lipid aggregates in the presence of monovalent or divalent cations is also perceived at the water level. It should also be pointed out that at very high temperatures the amount of isotropic water (the area of the isotropic line) dominates the spectrum in the presence of monovalent cations, whereas the converse is true with divalent cations. Of special interest is the fact that at 72°C, in the presence of Ca^{2+}, all the water is anisotropic, as it was in the bicelle domain, i.e., some 35°C lower. We have no electron micrographs taken from such temperatures, but both the ^{31}P NMR and the ^{2}H NMR of chains indicate that the system is macroscopically aligned (bilayer normal perpendicular to the field). So it seems that a new system with macroscopic orienting properties akin to bicelles is formed. It is clear that such a system demands a better characterization, which was beyond the scope of the present study.

CONCLUSION

We have shown in the present paper that biologically interesting cations can modulate the bicelle size and promote very interesting orientation properties. Because the concentrations at which such effects are obtained lie in the biologically relevant 50–200-mM range, care should be taken when adding negatively charged lipids or proteins that come along with their counterions. The optimum salt concentration may thus be already reached with these endogenous salts.

We are grateful to Dr. Gilles Moreau for enlightening explanations on torus geometry.

REFERENCES

Boroske, E., and W. Helfrich. 1978. Magnetic anisotropy of egg lecithin membranes. *Biophys. J.* 24:863–868.

Büldt, G., H. U. Gally, J. Seelig, and G. Zaccai. 1979. Neutron diffraction studies on phosphatidylcholine model membranes. I. Head group conformation. *J. Mol. Biol.* 134:673–691.

Burnett, L. J., and B. H. Müller. 1971. Deuteron quadrupolar coupling constants in three solid deuterated paraffin hydrocarbons: C_2D_6, C_4D_{10}, C_6D_{14}. *J. Chem. Phys.* 55:5829–5831.

Davis, J. H., K. R. Jeffrey, M. Bloom, M. I. Valic, and T. P. Higgs. 1976. Quadrupolar echo deuteron magnetic resonance spectroscopy in ordered hydrocarbon chains. *Chem. Phys. Lett.* 42:390–394.

Douliez, J. P., A. Léonard, and E. J. Dufourc. 1995. A restatement of order parameters in biomembranes: calculation of C-C bond order parameters from C-D quadrupolar splittings. *Biophys. J.* 68:1727–1739.

Douliez, J. P., A. Léonard, and E. J. Dufourc. 1996. Conformational approach of DMPC *sn*-1 versus *sn*-2 chains and membrane thickness: an approach to molecular protrusion by solid state ^{2}H-NMR and neutron diffraction. *J. Phys. Chem.* 100:18450–18457.

Engel, A. K., and D. Cowburn. 1981. The origin of multiple quadrupole couplings in the deuterium NMR spectra of the 2 chain of 1,2 dipalmitoyl-*sn*-glycero-3-phosphorylcholine. *FEBS Lett.* 126:169–171.

Faure, C., L. Bonakdar, and E. J. Dufourc. 1997. Determination of DMPC hydration in the L_α and L_β phases by ^{2}H solid state NMR of D_2O. *FEBS Lett.* 405:263–266.

Gabriel, E. N., and M. F. Roberts. 1984. Spontaneous formation of stable unilamellar vesicles. *Biochemistry.* 23:4011–4015.

Gabriel, E. N., and M. F. Roberts. 1986. Interaction of short-chain lecithin with long-chain phospholipids: characterization of vesicles that form spontaneously. *Biochemistry.* 25:2812–2821.

Gaemers, S., and A. Bax. 2001. Morphology of three lyotropic liquid crystalline biological NMR media studied by translational diffusion anisotropy. *J. Am. Chem. Soc.* 123:12343–12352.

Glover, K. J., J. A. Whiles, G. Wu, N. Yu, R. Deems, J. O. Struppe, R. E. Stark, E. A. Komives, and R. E. Vold. 2001. Structural evaluation of phospholipid bicelles for solution state studies of membrane-associated biomolecules. *Biophys. J.* 81:2163–2171.

Hauser, H., I. Pascher, R. H. Pearson, and S. Sundell. 1981. Preferred conformation and molecular packing of phosphatidylethanolamine and phosphatidylcholine. *Biochim. Biophys. Acta.* 650:21–51.

Katsaras, J., R. L. Donaberger, I. P. Swainson, D. C. Tennant, Z. Tun, R. R. Vold, and R. S. Prosser. 1997. Rarely observed phase transitions in a novel lyotropic liquid crystal system. *Phys. Rev. Lett.* 78:899–902.

Léonard, A., C. Escrive, M. Laguerre, E. Pebay-Peyroula, W. Néri, T. Pott, J. Katsaras, and E. J. Dufourc. 2001. Location of cholesterol in DMPC membranes: a comparative study by neutron diffraction and molecular mechanics simulation. *Langmuir.* 17:2019–2030.

Losonczi, J. A., and J. H. Prestegard. 1998. Improved dilute bicelle solutions for high resolution NMR of biological macromolecules. *J. Biomol. NMR.* 12:447–451.

Nieh, M. P., C. J. Glinka, and S. Krueger. 2001. SANS study of the structural phases of magnetically alignable lanthanide doped phospholipid mixtures. *Langmuir.* 17:2629–2638.

Picard, F., M. J. Paquet, J. Levesque, A. Bélanger, and M. Auger. 1999. ^{31}P NMR first spectral moment study of the partial magnetic orientation of phospholipid membranes. *Biophys. J.* 77:888–902.

Pott, T., and E. J. Dufourc. 1995. Action of melittin on the DPPC-cholesterol liquid-ordered phase: a solid state ^{2}H and ^{31}P NMR study. *Biophys. J.* 68:965–977.

Pott, T., J. C. Maillet, and E. J. Dufourc. 1995. Effects of pH and cholesterol on DMPA membranes: a solid state ^{2}H and ^{31}P NMR study. *Biophys. J.* 69:1897–1908.

Prosser, S. R., S. A. Hunt, J. A. DiNatale, and R. R. Vold. 1996. Magnetically aligned membrane model systems with positive order parameters: switching the sign of Szz with paramagnetic ions. *J. Am. Chem. Soc.* 118:269–270.

Prosser, S. R., V. B. Volkov, and I. V. Shiyanovskaya. 1998. Novel chelate-induced magnetic alignment of biological membranes. *Biophys. J.* 75:2163–2169.

Raffard, G., S. Steinbruckner, A. Arnold, J. H. Davis, and E. J. Dufourc. 2000. Temperature-composition diagram of dimyristoyl-dicaproyl phosphatidylcholine "bicelles" self-orienting in the magnetic field: a solid state ^{2}H- and ^{31}P-NMR study. *Langmuir.* 16:7655–7662.

Rance, M., I. C. P. Smith, and H. C. Jarrell. 1983. The effect of headgroup class on the conformation of membrane lipids in *Acholeplasma laidlawii*: a ^{2}H-NMR study. *Chem. Phys. Lipids.* 32:57–71.

Sanders, C. R., and J. H. Prestegard. 1990. Magnetically orientable phospholipid bilayers containing small amounts of a bile salt analogue, CHAPSO. *Biophys. J.* 58:447–460.

Sanders, C. R., and J. P. Schwonek. 1992. Characterization of magnetically orientable bilayers in mixtures of dihexanoylphosphatidylcholine and dimyristoylphosphatidylcholine by solid state NMR. *Biochemistry.* 31: 8898–8905.

Scholz, F., E. Boroske, and W. Helfrich. 1984. Magnetic anisotropy of lecithin membranes: a new anisotropy susceptometer. *Biophys. J.* 45: 589–592.

Sternin, E., D. Nizza, and K. Gawrisch. 2001. Temperature dependence of DMPC/DHPC mixing in bicellar solution and its structural implications. *Langmuir.* 17:2610–2616.

Vold, R. R., and S. R. Prosser. 1996. Magnetically oriented phospholipid bilayered micelles for structural studies of polypeptides: does the ideal bicelle exist? *J. Magn. Reson. Ser. B.* 113:267–271.